Photoswitching-Enabled Contrast Enhancement in Light Sheet Fluorescence Microscopy

Vettenburg, Tom; Corral, Angélica; Rodríguez-Pulido, Alberto; Flors, Cristina; Ripoll, Jorge

DOI:
10.1021/acsphotonics.6b00838

Publication date:
2017

Document Version
Peer reviewed version

Photoswitching-enabled Contrast Enhancement in Light Sheet Fluorescence Microscopy

Tom Vettenburg[1*], Angélica Corral[1], Alberto Rodríguez-Pulido[2], Cristina Flors[2], and Jorge Ripoll[1,3]

[1] Department of Bioengineering and Aerospace Engineering, Universidad Carlos III de Madrid, 28911 Madrid, Spain

[2] Madrid Institute for Advanced Studies in Nanoscience (IMDEA Nanociencia), C/Faraday 9, 28049 Madrid, Spain

[3] Experimental Medicine and Surgery Unit, Instituto de Investigación Sanitaria del Hospital Gregorio Marañón, 28007 Madrid, Spain

ABSTRACT: Light sheet fluorescence microscopy enables high resolution imaging of thick biological samples. By restricting the fluorescence excitation to a single plane, rapid wide-field image acquisition is possible with minimal sample exposure. Although light sheet microscopy is able to resolve sub-cellular features at depth in model organisms, elevated levels of endogenous auto-fluorescence often preclude acceptable contrast and may obscure features of interest in general samples. Here we demonstrate how photoswitchable fluorophores can be exploited to boost contrast in light sheet microscopy. The novel detection method enables high specificity while maintaining the optical sectioning capability of the light sheet microscope. Our experiments reveal structures hidden well below the ambient fluorescent background level by enhancing the contrast by two orders of magnitude.

KEYWORDS: light sheet microscopy, photo-switching, optical lock-in detection, auto-fluorescence, intensity evolution

Even if the light sheet microscope's history can be traced back to the beginning of the previous century[1], its adaptation for fluorescence imaging[2-4], and consequent rapid evolution is relatively recent[5-13]. Light sheet fluorescence microscopy has found wide-spread use in developmental biology by virtue of its ability to image thick three-dimensional specimens with high resolution and minimal sample irradiation. The associated low likelihood of photo-toxicity and premature photo-bleaching enables time-lapse studies over prolonged periods of time. Yet, as with other forms of fluorescence microscopy, elevated levels of endogenous auto-fluorescence often hamper contrast and may even prevent the identification of structures of interest. Hyper-spectral image acquisition followed by computational separation may be used when the emission spectra of the auto-fluorescence are sufficiently different from those of interest[14,15]. However powerful, such methods cannot distinguish spectra that are too similar. Here we demonstrate that, with minimal modifications, a light sheet microscope can be made robust to elevated levels of background fluorescence by relying on the switching dynamics of photoswitchable dyes. This enables us to distinguish fluorophores with identical spectra, including those caused by activation laser excitation.

Unlike regular fluorophores, photoswitchable dyes can be reversibly cycled between fluorescent and dark states by illumination with activation light, typically using short wavelengths in the violet or ultra-violet bands[16-18]. This unique characteristic is best known for its use in super-resolution imaging, including in the context of light sheet fluorescence microscopy[19-21]. Perhaps less well known is that the properties of such dyes can also be leveraged to improve image contrast. Modulating the state of the photoswitchable dye at a given frequency and evaluating its emission against an internal reference or model makes it possible to distinguish it from non-switching dyes[22-29]. The optical lock-in detection (OLID) method has been used for example to highlight neurons in a live Xenopus embryo against the auto-fluorescence background of its muscle cells[22]. Although the sensitivity of this technique is shown to be excellent for wide-field microscopy, we found that applying the same principles to light sheet microscopy leads to sub-optimal contrast due to the loss of its optical sectioning capability. In this manuscript we propose an alternative, yet straightforward, detection scheme that maintains the optical sectioning capability while dramatically enhancing contrast in light sheet microscopy.

Modulation of photoswitchable fluorophores is achieved with a fluorescence excitation laser (dotted blue line, Fig. 1a) that continuously irradiates the sample plane, and an activation laser that periodically switches the fluorophores on (violet line in Fig. 1a). A digitally-scanned light sheet microscope[6], is adapted to acquire a short frame sequence with co-aligned activation and excitation lasers followed by a short sequence with only the excitation laser. The fluorescence emitted by the photoswitchable dye is proportional to the density of the fluorophores in the activated state (green curve in Fig. 1a). During the first phase, the activation phase, the fraction of activated fluorophores converges exponentially towards a steady state, after which in a second phase the fluorophores are deactivated by the excitation laser. Although in principle a few cycles are sufficient for our purpose, this process is reversible and, if needed, can be repeated for hundreds of cycles[30].

The OLID method correlates the fluorescence intensity sequence recorded at each pixel with that of a small reference area that is known to contain only photoswitchable dye. The cross-correlation values can be expected to be

zero for pixels that correspond to a sample region free of photoswitching dye, while the values approach 1 for the case that only photoswitchable dye is present. The OLID image is represented by the positive per-pixel cross-correlation values.

By normalizing both the reference and the sequence for each pixel, even a very weak signal can be amplified and detected while largely removing the impact of variable or inhomogeneous illumination. Although this method has been demonstrated to significantly enhance contrast in a wide-field microscope set-up, it should be noted that selective, and thus inhomogeneous, illumination is the primary advantage of the light sheet microscope. Furthermore, the availability of a reliable reference in the sample volume complicates its practical use in light sheet microscopy.

The homogenization of the illumination is avoided by methods such as quantitative optical lock-in detection (qOLID)[29], and Synchronously Amplified Fluorescence Image Recovery (SAFIRe)[24,28]. The former models the fluorescence emission as a combination of exponential transitions and determines the concentrations based on its variance and covariance. Instead, SAFIRe determines the amplitude of the harmonic component at the switching frequency. This has the advantage that it does not require the estimation of any model parameters and is thus truly reference free. Both methods effectively remove the influence of relatively constant autofluorescence emission; however, neither model accounts for autofluorescence excited by the periodically switching activation laser. Such emission would result in a periodic square-wave modulation as seen in Figure 1c, which would be confused with photoswitching (Fig. 1b). In general, a measurement will be an *a priori* unknown combination of switching and non-switching signals.

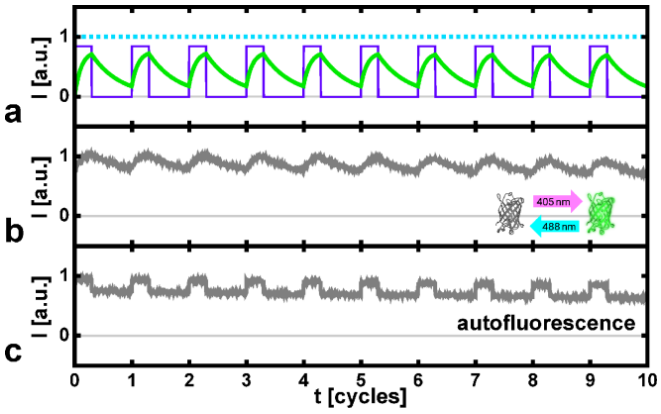

Figure 1. Imaging principle and effect of the activation light sheet on different emitters. (**a**) Illumination sequences of the imaging process. The excitation intensity is constant as indicated by the dotted blue line. The solid violet line indicates the activation laser intensity, which is switched on in the first phase and switched off during the second phase of each cycle. The thick green line indicates the fluorescence emission, proportional to the number of activated fluorophores. The intensities are scaled independently for clarity. (b-c) Simulated fluorescence emission from two different points in the same sample. (**b**) Fluorescence emission of photoswitchable fluorophore against a non-switching background. (**c**) In general, the intensity measured in absence of photoswitching may exhibit a square wave modulation due to autofluorescence excited by the activation laser.

Due to the relatively low, sample friendly, powers typically used in light sheet microscopy, the reversible transitions between the on and off state do not saturate exponentially. Instead of correlating each sequence with a model or reference signal, we introduce an alternative algorithm that tracks the fluorescence signal evolution within the activation phase and the deactivation phase separately. The emission from photoswitchable dyes should increase during the activation phase, and decrease again during the deactivation phase after switching off the activation laser. Conversely, non-switching (auto)-fluorescence or scattered laser light would result in a nearly constant intensity measurement within each phase. A gradual long-term variation can still be expected due to e.g. photo-bleaching. We therefore determine what we refer to as the Intensity Evolution as the difference of the slope of the per-pixel intensity in the activation phase and that in the deactivation phase (see Supplementary Information S1, Fig. S1). Although the mean intensity in both phases may be different due to autofluorescence or laser scattering, the slope should tend to zero, and hence also the Intensity Evolution. On the other hand, photoswitching manifests itself as a positive intensity slope during the activation phase and a negative slope during the deactivation phase, thus combining to a large Intensity Evolution value.

In what follows we demonstrate how the Intensity Evolution successfully achieves high contrast imaging in the presence of elevated levels of fluorescent background. To that end we constructed a digitally scanned light sheet microscope with photoswitching capability. The proposed method is shown to be highly specific and robust to modulations of the auto-fluorescence. Finally, we discuss how the novel algorithm maintains the optical sectioning capability, a central pillar of light sheet microscopy.

RESULTS AND DISCUSSION

We evaluate the performance of the Intensity Evolution method and compare it to conventional light sheet microscopy, OLID, and SAFIRe. Figure 2 shows images of a sample containing both non-switching and reversibly photoswitching fluorescent microspheres immobilized in agarose. The latter are prepared by coating functionalized micro-spheres with the photoswitchable fluorescent protein rsEGFP as detailed in the Supplementary Information S3.3. This protein can be reversibly activated using low power irradiation at a wavelength of 405 nm, while fluorescence excitation with a wavelength of 491 nm causes deactivation at a relatively slow rate[30].

A time sequence of 10 cycles was recorded for a selected plane in the sample, and evaluated using three different contrast enhancement methods. Figure 2a shows the time-averaged intensity per pixel as would be obtained by a conventional light sheet microscope. Figure 2b shows the same data after OLID. It can be noted that, while the non-switching microsphere on the right hand side is well suppressed, the four photo-switchable microspheres become prominent. At the same time, as an indication of its sensitivity to weak signals, an out-of-focus structure clouds the bottom left of the image. Figure 2c shows the less noisy image obtained by the SAFIRe method. Although this

method suppresses the background and results in high contrast, the non-switching microsphere indicated by the white arrow is incorrectly recognized as photoswitching. This can be explained by a relatively weak fluorescence excitation of the non-switching microspheres by the activation laser, which produces a square wave modulation that is mistaken for photoswitching. Figure 2d demonstrates how the Intensity Evolution combines contrast enhancement with specificity towards the photoswitching response of rsEGFP. The four photoswitching microspheres appear bright, while the signal of the non-switching sphere is well suppressed.

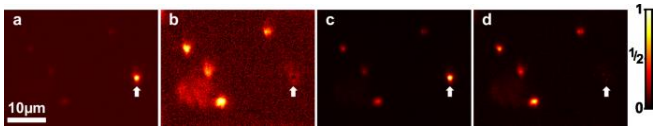

Figure 2. Comparison of different modulation contrast enhancement algorithms with microspheres (ø 1 µm), either conventional fluorescent or coated with the reversibly photoswitching rsEGFP. (**a**) The time-averaged intensity image as for a conventional light sheet microscope. All but one emitter shows photoswitching behavior except for the right-most microsphere indicated by an arrow. (**b**) Optical lock-in detection (OLID) image. (**c**) Fourier component amplitude (SAFIRe), (**d**) Intensity Evolution. For clarity, all images are scaled to the maximum intensity value.

Figure 3 shows an optical section of a sample containing HaCaT (aneuploid immortal keratinocyte) cells expressing EGFP, and *E. coli* bacteria expressing the photoswitchable rsEGFP. As the fluorescence spectra are practically identical, a conventional light sheet image cannot distinguish between the emission of both green fluorophores (Fig. 3a). However, the Intensity Evolution, determined from the same data, correctly highlights only the bacteria in the sample. Figure 3b shows a superposition of the Intensity Evolution on the conventional image in magenta as a reference. It now becomes clear that the point-like emitter near the top right of the cell membrane is indeed a bacterium expressing the photoswitchable fluorophore. A diagonal cross section of the intensity evolution image shows that the non-switching fluorescence of the cell is effectively blocked, while a high contrast peak is visible at the position of the bacterium (Fig. 3c, thin green line), highlighting the specificity of the method.

We demonstrate the robustness of the method for the case of a dominant fluorescent background that drowns out the fluorescence of the photoswitchable dye of interest. Figure 4 compares the results for a sample of microspheres coated with photoswitchable rsEGFP that are suspended in agarose gel with the very high concentration of 2 µM of Alexa488 to simulate an extreme auto-fluorescence background. Figure 4a shows a slice of the suspension as seen by a conventional light sheet microscope. Without deeper analysis, the nearly uniform high intensity hides any evidence of embedded microspheres. However, as seen in Figure 4c, the per-phase Intensity Evolution of 20 cycles reveals the presence of microspheres labeled with rsEGFP.

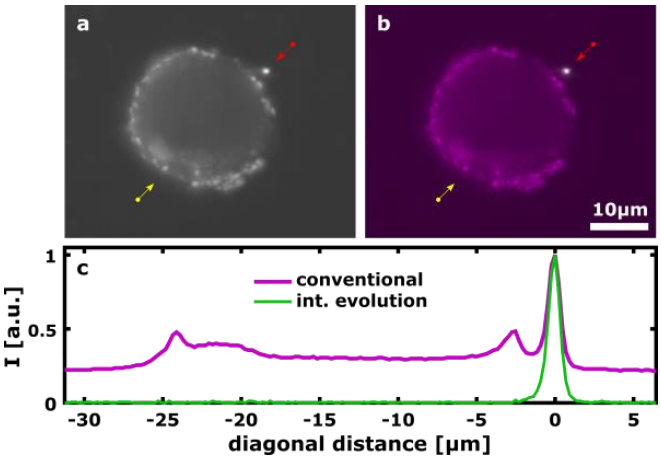

Figure 3. Optical section of an HaCaT (aneuploid immortal keratinocyte) cell expressing regular EGFP and an *E. coli* bacterium expressing rsEGFP. (a) A conventional time-averaged image. (b) The Intensity Evolution super-imposed on the conventional image in magenta. Although both the bacterium and keratinocyte emit fluorescence with a nearly identical green spectrum, the Intensity Evolution highlights the bacterium. (c) A cross section of the conventional image (thick magenta line) and the intensity evolution image (thin green line), diagonally through the cell and bacterium from the yellow until the red marker overlaid in panel (a) and (b). Both are normalized to their maximum value.

Closer inspection of that data of Figure 4a shows that the intensity at the position of the top left microsphere is oscillatory and actually 0.03 times lower than that of the surrounding areas. In contrast, the intensity at the microspheres is 14 times larger than the background in the Intensity Evolution shown in Figure 4c, a more than 400-fold improvement.

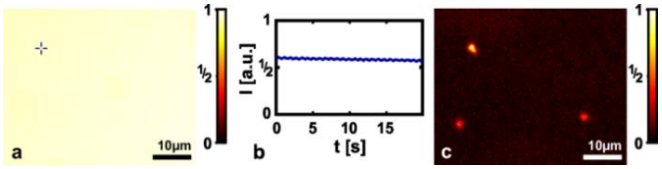

Figure 4. Microspheres labeled with the reversibly switchable protein rsEGFP suspended in 0.5% agarose gel with a high concentration (2 µM) of Alexa488 dye. (**a**) The conventional light sheet image calculated as a per-pixel time-integration. The image is almost uniform due to the high concentration of Alexa488 dye. (**b**) The average intensity in a 3×3-pixel area is plotted as a function of time. This signal corresponds to the position indicated by the blue cross-hair in (a); however, the conventional image has insufficient contrast (-3%) to discern it clearly. (**c**) The Intensity Evolution, revealing the photoswitchable microspheres.

We investigate the optical sectioning capability of the Intensity Evolution. To that end we recorded a stack of image sequences at different depths, *z*, in the sample. Figure 5a-c show axial sections of a point-like photoswitchable emitter, for conventional light sheet microscopy (a), and processed by the optical lock-in (b), and Intensity Evolution (c), respectively.

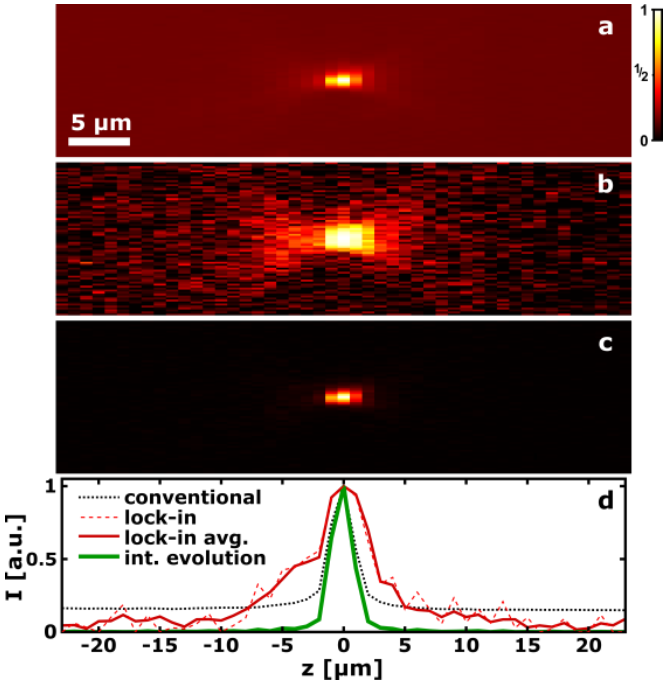

Figure 5. A volume acquired around a photoswitchable emitter. An axial section is shown without processing (**a**), and after processing using OLID (**b**), and with the Intensity Evolution (**c**). (**d**) The intensity along a *z*-axis of the conventional light sheet image (dotted black), the optical lock-in light sheet image (dashed red), as well as the average of a 3×3 pixel area around the z-axis (thick solid red), and the Intensity Evolution (solid green). For clarity, all plots and images are normalized to the maximum intensity.

To facilitate comparison, cross sections at $x \equiv y \equiv 0$ are plotted in Figure 5d. It can be seen that the conventional light sheet provides good sectioning with a full-width-at-half-maximum (FWHM) of 2.8 µm however, the intensity does not reach near-zero values because the light sheet is considerably larger than the depth-of-focus to accommodate a large field-of-view. It is clear from Figure 5b that the high sensitivity of the optical lock-in correlation has the side effect of introducing noise in dark out-of-focus areas of the sample. Also a severe reduction in the optical sectioning capability of the light sheet microscope as can be seen in Figure 5d (dashed red), where the FWHM of the optical lock-in cross section is 5.5 µm, twice that of the conventional light sheet cross section. While the selective illumination of the lightsheet is concentrated near the focal plane, some residual light may reach molecules on both sides of the focal plane. The normalization in the Pearson's product of the optical lock-in algorithm effectively compensates for the reduced excitation in those out-of-focus areas of the sample, thereby reducing the spatial selectivity of the light sheet microscope. The compensation also increases the noise level at planes where the emitter is not in focus; however, that has no appreciable effect on the section width as can be seen by reducing the noise influence by averaging over a 3×3 pixel area around the axis (Fig. 5d, solid red). The signal obtained using the Intensity Evolution is dependent on both the activation and the excitation intensity at a given location in the sample. The combined effect can be noticed as the marked contrast improvement seen in Figure 5c and Figure 5d (solid green). The Intensity Evolution confines the photoswitching to a region near the origin with a FWHM of 2.1 µm, about 25% less than that of the conventional light sheet image.

In conclusion, photoswitchable fluorophores can significantly enhance light sheet microscopy contrast in the presence of a strong background, crucially, while maintaining the optical sectioning capability. This novel method was able to increase the contrast by a factor of 400 in the presence of high levels of background fluorescence, and has the potential to reveal biological features in highly autofluorescent samples. Moreover, it has now become possible to distinguish photoswitchable fluorophores from fluorophores with practically identical spectra. This enables co-localization studies without the need to switch filters or excitation laser wavelength.

ASSOCIATED CONTENT

Supporting Information

A description of the optical set up, image calculation, and sample preparation can be found in the Supporting Information below.

AUTHOR INFORMATION

Corresponding Author

*E-mail: tom.vettenburg@uc3m.es (T. Vettenburg).

Author Contributions

C.F. and T.V. conceived the experiments. T.V. and J.R. constructed the light sheet microscope. A. C., C.F. and A. R.-P. prepared the samples. T.V. wrote the control software and analyzed the results. All authors reviewed the manuscript.

Note

The authors declare no competing financial interests.

ACKNOWLEDGMENTS

This research was supported by the European Union's Seventh Framework Programme (FP7/2007-2013) under the grants FP7-PEOPLE-2013-IEF-622643, FP7-PEOPLE-2011-CIG-303620 and FP7-PEOPLE-2011-COFUND-291803, the Royal Society of London International Exchange Scheme grant IE120848, and by the Spanish *Ministerio de Economía y Competitividad* grants RyC2011-07637, MAT2015-66605-P, and FIS2013-41802-R.

REFERENCES

(1) Siedentopf, H.; Zsigmondy, R. Über sichtbarmachung und groessenbestimmung ultramikroskopischer teilchen, mit besonderer anwendung auf goldrubinglaesern. Annalen der Physik 315, **1902,** 1–39.

(2) Voie, A. H. Imaging the intact guinea pig tympanic bulla by orthogonal-plane fluorescence optical sectioning microscopy. Hearing Research **2002,** 171, 119–128.

(3) Huisken, J.; Swoger, J.; Bene, F. D.; Wittbrodt, J.; Stelzer, E. H. K. Optical sectioning deep inside live embryos by selective plane illumination microscopy. Science **2004,** 305, 1007–1009.

(4) Santi, P. A.; Johnson, S. B.; Hillenbrand, M.; Grandpre, P. Z.; Glass, T. J.; Leger, J. R. Thin-sheet laser imaging microscopy for optical sectioning of thick tissues. BioTechniques **2009,** 46, 287–294.

(5) Huisken, J.; Stainier, D. Y. R. Even fluorescence excitation by multidirectional selective plane illumination microscopy (mSPIM). Opt. Lett. **2007,** 32, 2608–2610.
(6) Keller, P. J.; Schmidt, A. D.; Wittbrodt, J.; Stelzer, E. H. K. Reconstruction of zebrafish early embryonic development by scanned light sheet microscopy. Science **2008,** 322, 1065–1069.
(7) Huisken, J.; Stainier, D. Y. R. Selective plane illumination microscopy techniques in developmental biology. Development **2009,** 136, 1963–1975.
(8) Gao, L.; Shao, L.; Higgins, C. D.; Poulton, J. S.; Peifer, M.; Davidson, M. W.; Wu, X.; Goldstein, B.; Betzig, E. Noninvasive imaging beyond the diffraction limit of 3D dynamics in thickly fluorescent specimens. Cell **2012,** 151, 1370–1385.
(9) Fahrbach, F. O.; Voigt, F. F.; Schmid, B.; Helmchen, F.; Huisken, J. Rapid 3D light-sheet microscopy with a tunable lens. Opt. Express **2013,** 21, 21010.
(10) Vettenburg, T.; Dalgarno, H. I. C.; Nylk, J.; Lladó, C. C.; Ferrier, D. E. K.; Čižmár, T.; Gunn-Moore, F. J.; Dholakia, K. Light sheet microscopy using an airy beam. Nat. Methods 11, **2014,** 541–544.
(11) Chen, B.-C.; Legant, W. R.; Wang, K.; Shao, L.; Milkie, D. E.; Davidson, M. W.; Janetopoulos, C.; Wu, X. S.; Hammer, J. A.; Liu, Z.; English, B. P.; Mimori-Kiyosue, Y.; Romero, D. P.; Ritter, A. T.; Lippincott-Schwartz, J.; Fritz-Laylin, L.; Mullins, R. D.; Mitchell, D. M.; Bembenek, J. N.; Reymann, A.-C.; Böhme, R.; Grill, S. W.; Wang, J. T.; Seydoux, G.; Tulu, U. S.; Kiehart, D. P.; Betzig, E. Lattice light-sheet microscopy: Imaging molecules to embryos at high spatiotemporal resolution. Science **2014,** 346.
(12) Chhetri, R. K.; Amat, F.; Wan, Y.; Höckendorf, B.; Lemon, W. C.; Keller, P. J. Whole-animal functional and developmental imaging with isotropic spatial resolution. Nat. Methods **2015,** 12, 1171–1178.
(13) Fu, Q.; Martin, B. L.; Matus, D. Q.; Gao, L. Imaging multicellular specimens with real-time optimized tiling light-sheet selective plane illumination microscopy. Nat. Commun. **2016,** 7, 11088.
(14) Jahr, W.; Schmid, B.; Schmied, C.; Fahrbach, F. O.; Huisken, J. Hyperspectral light sheet microscopy. Nat. Commun. **2015,** 6, 7990–.
(15) Lavagnino, Z.; Dwight, J.; Ustione, A.; Nguyen, T.-U.; Tkaczyk, T. S.; Piston, D. W. Snapshot hyperspectral light-sheet imaging of signal transduction in live pancreatic islets. Biophysical Journal **2016,** 111, 409–417.
(16) Tian, Z.; Li, A. D. Q. Photoswitching-enabled novel optical imaging: Innovative solutions for real-world challenges in fluorescence detections. Accounts of Chemical Research **2013,** 46, 269–279.
(17) Chozinski, T. J.; Gagnon, L. A.; Vaughan, J. C. Twinkle, twinkle little star: Photoswitchable fluorophores for super-resolution imaging. FEBS Letters **2014,** 588, 3603–3612.
(18) Patterson, G. H. Highlights of the optical highlighter fluorescent proteins. Journal of Microscopy **2011,** 243, 1–7.
(19) Zanacchi, F. C.; Lavagnino, Z.; Donnorso, M. P.; Bue, A. D.; Furia, L.; Faretta, M.; Diaspro, A. Live-cell 3D super-resolution imaging in thick biological samples. Nat. Methods **2011,** 8, 1047–1049.
(20) Li, D.; Shao, L.; Chen, B.-C.; Zhang, X.; Zhang, M.; Moses, B.; Milkie, D. E.; Beach, J. R.; Hammer, J. A.; Pasham, M.; Kirchhausen, T.; Baird, M. A.; Davidson, M. W.; Xu, P.; Betzig, E. Extended-resolution structured illumination imaging of endocytic and cytoskeletal dynamics. Science **2015,** 349.
(21) Hoyer, P.; de Medeiros, G.; Balázs, B.; Norlin, N.; Besir, C.; Hanne, J.; Kräusslich, H.-G.; Engelhardt, J.; Sahl, S. J.; Hell, S. W.; Hufnagel, L. Breaking the diffraction limit of light-sheet fluorescence microscopy by RESOLFT. Proc. Natl. Acad. Sci. U.S.A. **2016,** 113, 3442–3446.
(22) Marriott, G.; Mao, S.; Sakata, T.; Ran, J.; Jackson, D. K.; Petchprayoon, C.; Gomez, T. J.; Warp, E.; Tulyathan, O.; Aaron, H. L.; Isacoff, E. Y.; Yan, Y. Optical lock-in detection imaging microscopy for contrast-enhanced imaging in living cells. Proc. Natl. Acad. Sci. U.S.A. **2008,** 105, 17789–17794.
(23) Mao, S.; Benninger, R. K.; Yan, Y.; Petchprayoon, C.; Jackson, D.; Easley, C. J.; Piston, D. W.; Marriott, G. Optical lock-in detection of FRET using synthetic and genetically encoded optical switches. Biophysical Journal **2008,** 94, 4515 – 4524.
(24) Richards, C. I.; Hsiang, J.-C.; Senapati, D.; Patel, S.; Yu, J.; Vosch, T.; Dickson, R. M. Optically modulated fluorophores for selective fluorescence signal recovery. J. Am. Chem. Soc. **2009,** 131, 4619–4621.
(25) Smith, D. A.; Holliger, P.; Flors, C. Reversible fluorescence photoswitching in DNA. The Journal of Physical Chemistry B **2012,** 116, 10290–10293.
(26) Yao, J.; Shcherbakova, D. M.; Li, C.; Krumholz, A.; Lorca, R. A.; Reinl, E.; England, S. K.; Verkhusha, V. V.; Wang, L. V. Reversibly switchable fluorescence microscopy with enhanced resolution and image contrast. J. Biomed. Opt. **2014,** 19, 086018.
(27) Chen, Y.-C.; Jablonski, A. E.; Issaeva, I.; Bourassa, D.; Hsiang, J.-C.; Fahrni, C. J.; Dickson, R. M. Optically modulated photoswitchable fluorescent proteins yield improved biological imaging sensitivity. J. Am. Chem. Soc. **2015,** 137, 12764–12767.
(28) Querard, J.; Markus, T.-Z.; Plamont, M.-A.; Gauron, C.; Wang, P.; Espagne, A.; Volovitch, M.; Vriz, S.; Croquette, V.; Gautier, A.; Le Saux, T.; Jullien, L. Photoswitching kinetics and phase-sensitive detection add discriminative dimensions for selective fluorescence imaging. Angewandte Chemie International Edition **2015,** 54, 2633–2637.
(29) Abbandonato, G.; Storti, B.; Signore, G.; Beltram, F.; Bizzarri, R. Quantitative optical lock-in detection for quantitative imaging of switchable and non-switchable components. Microscopy Research and Technique **2016,** 79, 929–937.
(30) Grotjohann, T.; Testa, I.; Leutenegger, M.; Bock, H.; Urban, N. T.; Lavoie-Cardinal, F.; Willig, K. I.; Eggeling, C.; Jakobs, S.; Hell, S. W. Diffraction-unlimited all-optical imaging and writing with a photochromic GFP. Nature **2011,** 478, 204–208.

Table of Contents artwork

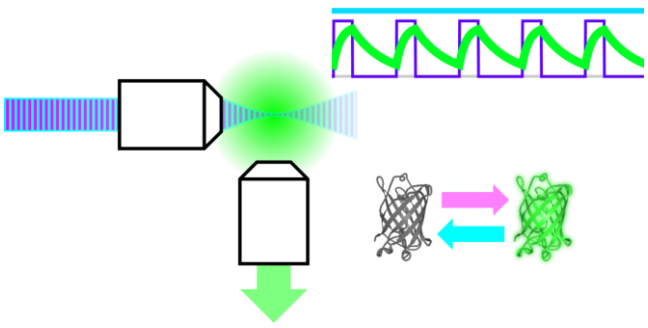

Supporting Information: Photoswitching-enabled Contrast Enhancement in Light Sheet Fluorescence Microscopy

Tom Vettenburg[1*], Angélica Corral[1], Alberto Rodríguez-Pulido[2], Cristina Flors[2], and Jorge Ripoll[1,3]

[1]Department of Bioengineering and Aerospace Engineering, Universidad Carlos III de Madrid, 28911 Madrid, Spain
[2]Madrid Institute for Advanced Studies in Nanoscience (IMDEA Nanociencia), C/Faraday 9, 28049 Madrid, Spain
[3]Experimental Medicine and Surgery Unit, Instituto de Investigación Sanitaria del Hospital Gregorio Marañón, 28007 Madrid, Spain

ABSTRACT

Light sheet fluorescence microscopy enables high resolution imaging of thick biological samples. By restricting the fluorescence excitation to a single plane, rapid wide-field image acquisition is possible with minimal sample exposure. Although light sheet microscopy is able to resolve sub-cellular features at depth in model organisms, elevated levels of endogenous auto-fluorescence often preclude acceptable contrast and may obscure features of interest in general samples. Here we demonstrate how photoswitchable fluorophores can be exploited to boost contrast in light sheet microscopy. The novel detection method enables high specificity while maintaining the optical sectioning capability of the light sheet microscope. Our experiments reveal structures hidden well below the ambient fluorescent background level by enhancing the contrast by two orders of magnitude.

S1 Intensity Evolution image calculation

The Intensity Evolution is calculated on a per pixel basis as the difference between the slopes in the activation phases and those in deactivation phases (see Fig. S1). The slopes within each phase are determined independently from a linear root-mean-square minimizing fit of the measured intensity time series.

The Intensity Evolution algorithm is relatively straightforward to implement. The following listing gives an example implementation in GNU Octave of both the optical lock-in detection method, `calcOLID`, and the Intensity Evolution method, `calcIntEv`. It starts with an example demonstrating the algorithm implementation and displays the output images next to the conventional light sheet image. Both the activation and the deactivation phase are maintained for 5 frames and 10 cycles with a photo-switching point-emitter at the center of a two-dimensional region of interest.

```
function supplementaryCode()
    % Obtain the data
    [rawData,reference,nbOnFrames,nbOffFrames]=getData();

    % Process using different methods
    conventionalImg = calcConventional(rawData);
    olidImg = calcOLID(rawData, reference);
    ieImg = calcIntEv(rawData, nbOnFrames, nbOffFrames);

    % Display
    figure;
    colormap(hot);
    ax(1) = subplot(2,3,1);
    imagesc(conventionalImg); title('Conventional');
    axis equal tight off;
    ax(2) = subplot(2,3,2);
    imagesc(olidImg); title('OLID');
    axis equal tight off;
    ax(3) = subplot(2,3,3);
```

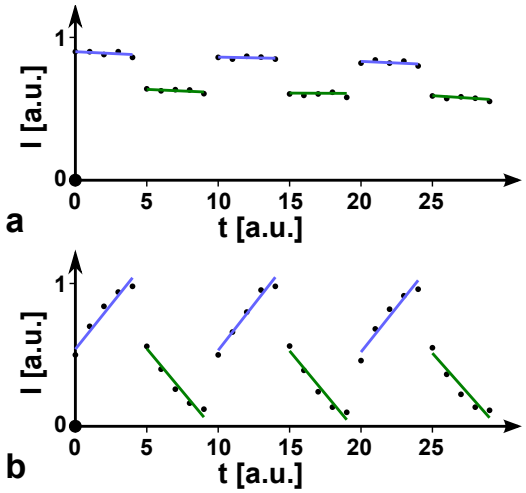

Figure S1 | Intensity evolution comparison of conventional fluorescence emission and that of photoswitchable molecules against an auto-fluorescent background. Five acquisitions are shown during the activation phase (405 nm laser on) and the deactivation phase (405 nm laser off) for three cycles. The per-phase linear fits are shown in blue for the activation phases and in green for the deactivation phases. Disregarding photo-bleaching, the excitation of auto-fluorescence does not change at the constant irradiation during the activation or deactivation phases (**a**). However, the fluorescence emission of photoswitchable fluorophores does show clear upward and downward trends within the respective phases (**b**).

```
    imagesc(ieImg); title('Intensity Evolution');
    axis equal tight off;
    subplot(2,3,[4:6]);
    plot([reference(:),...
        squeeze(rawData(1+floor(end/2),1+floor(end/2),:))]);
    xlabel('frame number');
    ylabel('I [a.u.]');
    legend({'OLID reference', 'actual emission'});

    linkaxes(ax);
end

%
% Returns the Conventional image
%
% Inputs:
%   rawData: the same set of frames used for the OLID
%   and Intensity Evolution calculations.
%
function conventionalImg = calcConventional(rawData)
    % Calculate the mean of all frames
    conventionalImg = mean(rawData,3);
end

%
% Returns the OLID image
%
% Inputs:
%   rawData: a set of frames
%   reference: vector with per frame intensity of
%   a reference photo-switcher
%
function olidImg = calcOLID(rawData, reference)
    inputSize = size(rawData);
    outputSize = inputSize(1:2);
    nbFrames = inputSize(3);

    % Calculate the mean and std outside the loop
    refMean = mean(reference);
    refStd = std(reference);
    dataMean = mean(rawData,3);
    dataStd = std(rawData,1,3);
    % Calculate the cross-correlation
    % page 2, doi: 10.1073/pnas.0808882105
    olidImg = zeros(outputSize);
    for frameIdx = 1:nbFrames,
        integrand = (reference(frameIdx)-refMean).*...
            (rawData(:,:,frameIdx)-dataMean)./...
            (refStd.*dataStd);
        olidImg = olidImg + integrand;
    end

    olidImg = max(0,olidImg);
end

%
% Returns the Intensity Evolution image
%
% Inputs:
%   rawData: a set of frames
%   nbOnFrames: frames per cycle activation was ON
%   nbOffFrames: frames per cycle activation was OFF
%
function ieImg = calcIntEv(rawData,nbOnFrames,nbOffFrames)
    inputSize = size(rawData);
    outputSize = inputSize(1:2);
    nbFrames = inputSize(3);
    nbFramesPerCycle = nbOnFrames+nbOffFrames;
    nbCycles = nbFrames/nbFramesPerCycle;

    ieImg = zeros(outputSize);
    for cycleIdx = 1:nbCycles,
        % Split in ON and OFF phase
        onFrames = rawData(:,:,[1:nbOnFrames]+...
            nbFramesPerCycle*(cycleIdx-1));
        offFrames = rawData(:,:,...
            nbOnFrames+[1:nbOffFrames]+...
            nbFramesPerCycle*(cycleIdx-1));

        ieImg = ieImg + ...
            (calcSlopes(onFrames)-calcSlopes(offFrames));
    end
    ieImg = max(0,ieImg);
end
% Calculates the per-pixel slope of the data
function slopes = calcSlopes(data)
    % Convert data to matrix amenable to dot product
    inputSize = size(data);
    nbFrames = inputSize(3);
    data = reshape(data,[],nbFrames);
    % Calculate slopes of linear fit as dot product
    unitySlope = [0:(nbFrames-1)].'-((nbFrames-1)/2);
    slopes = data*unitySlope./sum(unitySlope.^2);
    % Convert back to image format
    slopes = reshape(slopes,inputSize(1:2));
end

%
% Returns a simulated data set for evaluation
%
function [rawData,reference,nbOnFrames,nbOffFrames]=getData()
    nbCycles = 10;
    nbOnFrames = 5;
    nbOffFrames = 5;
    frameSize = [25 25];

    % Create a synthetic reference signal
    actRate = 1/3;
    deactRate = 1/3;
    initial = 0;
    reference = [];
    for cycleIdx = 1:nbCycles,
        act = 1 - (1-initial)*exp(-actRate*[1:nbOnFrames]);
        deact = act(end)*exp(-deactRate*[1:nbOffFrames]);
        reference = [reference act deact];
        initial = deact(end);
    end

    % Simulate a photo switching emitter at the center of
    % an auto-fluorescent region of equal average intensity
    rawData = mean(reference)*...
        ones([frameSize, (nbOnFrames+nbOffFrames)*nbCycles]);
    % place photo-switcher in the center
    rawData(1+floor(end/2),1+floor(end/2),:) = reference;
    % and calculate photon noise and detector noise
    rawData = poissrnd(rawData.*1000)./1000;
end
```

Prior to the image calculation, the recorded image frames are registered to prevent any errors due to sample drift using the algorithm described by Guizar-Sicairos et al.[1]. Sub-pixel image registration is performed on each two-dimensional slice of a three-dimensional data set. The first frame of all but the first z-slice is registered with the time-averaged registered image of the proceeding z-slice. All consecutive frames are registered to the average of the previous frames in that z-slice.

S2 Optical set-up and acquisition

Intermittent $\lambda = 405$ nm activation illumination and synchronized acquisition was achieved by adapting a conventional digitally-scanned light sheet fluorescence microscope. A water dipping objective (HCX APO L $40\times/0.80$ W U-V-I, Leica Microsystems GmbH, Germany) in combination with an infinity-corrected tube lens (ITL200, Thorlabs GmbH, Germany) images the sample's focal plane onto the sCMOS camera (Orca Flash 4.0 v2, Hamamatsu Photonics, Japan). An emission filter (525/45nm tech spec fluorescence filter #86-984, Edmund Optics Inc., USA) restricts transmission to a band around the peak of the green fluorescence emission.

A long working distance objective (PLAN APO ELWD $20\times/0.42$ WD$=20$ mm, Edmund Optics, USA) was used to illuminate the focal plane orthogonally through a microscope

	P_{act}	P_{exc}	Δt	n_c	n_{on}	n_{off}
Figure 2	106 μW	1.9 mW	50 ms	10	10	10
Figure 3	42 μW	3.8 mW	75 ms	25	5	5
Figure 4	204 μW	7.6 mW	80 ms	20	5	5
Figure 5	42 μW	3.0 mW	75 ms	10	5	5

Table S1 | Acquisition parameters.

cover glass enclosed, water-filled sample chamber. A spatial light modulator (LCOS X10468-01, Hamamatsu, Japan) in the light path is used to correct for aberrations and control the effective numerical aperture of the beams that form the light sheet over a programmable field-of-view. Both lasers (iBeam smart 405 and 488, TOPTICA Photonics AG, Germany) are focussed with an effective numerical aperture of 0.25 at a point in the focal plane. Consequently, galvanometer scanning mirrors (GVS012/M, Thorlabs GmbH, Germany), positioned conjugate to the back aperture of the illumination objective, are used to rapidly swipe the beam axis so that the field-of-view is illuminated homogeneously during the time of a single image acquisition. LabVIEW software was written to synchronize the activation laser, the galvanometer scanner, and the camera acquisition.

Table S1 lists the acquisition parameters used to produce all images. The columns list the activation power, P_{act}, and excitation power, P_{exc}, measured at the objective, the integration time of the camera, Δt, the number of cycles, n_c, and the number of frames per cycle during which the activation was on, n_{on}, and off, n_{off}, respectively.

S3 Sample preparation

S3.1 Preparation of HaCaT-EGFP cells

HaCaT cells, a spontaneously immortalized human keratinocyte cell line widely used for studies of skin biology and differentiation, were previously transfected by incubation with a recombinant EGFP-expressing LZR-based amphotropic retrovirus supernatant generated by transient transfection in 293T cells[2]. Before imaging in the light sheet microscope, the adherent cells were detached using trypsin and brought into suspension, after which 5 mL of prewarmed media (serum in the media inactivated trypsin) is added to the plate. One million cells were counted and resuspended in 50 µL of media DMEM containing 10% Fetal Bovine Serum (FBS). Next, we mixed the cells with 50 µL of 1% low melting agarose (SeaPlaque Agarose Cat. 50100, Lonza Group, Switzerland) at 37°C.

S3.2 Expression of rsEGFP in bacteria

Escherichia coli bacteria were prepared as described previously in the literature[3], with minor modifications to the protocol. The *E. coli* DH10β cultures expressing reversibly switchable enhanced green fluorescent protein (rsEGFP) (Abberior GmbH, Germany) in the cytosol were grown in LB broth containing 0.1 mg/mL ampicillin and IPTG as inducing agent, with gentle shaking at 200 rpm, at 37 °C for 24 hours. The bacteria were harvested after 5 min of centrifugation at 3500 g, washed twice in PBS and resuspended in the same buffer.

S3.3 Coating of microspheres with reversibly switchable fluorescent protein

Purified His-tagged rsEGFP (0.2 mg/mL) were incubated with 6 mg/mL HisPur Ni-NTA (nitrilotriacetic acid) magnetic beads (⌀1 µm, Thermo Scientific) in 400 µL PBS during 1 h at room temperature. The coated beads were collected with a magnet and the supernatant was discarded. The beads were washed 3× with PBS.

S3.4 Sample mounting

All samples were embedded in 0.5% agarose gel in phosphate-buffered saline (PBS). A mixture of commercially available green fluorescent microspheres (⌀1 µm, G0100, Duke Scientific) and the rsEGFP coated microspheres were sucked into an approximately 8 mm long and 0.8 mm-outer-diameter (FEP) tube (Bohlender GmbH, Germany) with the help of a micropipette. Biological samples were sucked with agarose into a 0.8 mm-inner-diameter glass capillary (BR708757, Blaubrand micropipettes, intraMark, 200 μL, Sigma-Aldrich Chemie GmbH, Germany), and lowered out the bottom end just before imaging. The samples were positioned in the water-filled sample chamber using motorized stages (PLS-85, PI miCos GmbH, Germany, and T-LSM025A and T-RSW60C, Zaber Technologies Inc., Canada).

S4 Evaluation of signal to background contrast

Light sheet microscopy is typically used on living organisms for which sample irradiation is kept to the minimum level required to yield what is deemed acceptable signal-to-noise. In the low-power regime the transitions of the reversible switchable fluorophore are approximately linear, making the Intensity Evolution the method of choice. However, the relatively low transition rates do lead to a limited modulation depth which may impact the image signal obtained.

In this section we investigate how the contrast of a photo-switchable source varies with respect to a constant background of equal average brightness. Such a sample would appear of uniform intensity in a conventional fluorescence image. The noise level depends on one hand on the activation level, and on the other hand on the label density, brightness, and the detection efficiency of the microscope. We thus separated both variables and simulated various transition rates as well as shot-noise for different photon counts at the saturation level of the fluorophores, n_{sat}. The intensity of the activation laser is assumed to be set so that the activation rate and deactivation rate are matched. Figure S2 shows the reference photo-switching intensity and the associated contrast for activation rates of 0.1, 0.5, and 1 per frame, for a maximum of 20 cycles with fluorophore activation during the first 5 frames of each cycle, followed by 5 frames without activation. The

contrast is calculated using only the first 5 cycles, the first 10, or all 20. As can be seen from Figure S2(b,d,f), usage of more cycles improves the contrast both for OLID (red lines) and for Intensity Evolution (green lines).

It can be noted that the signal-to-background ratio (SBR) of Intensity Evolution increases as the photon count increases and the noise decreases with respect to the signal. In contrast, the OLID value converges as the signal to noise increases with photon count. By comparing the plots in Figure S2(b,d,f), it can be noticed that, to some extent, the transition rate affects the Intensity Evolution method when changed from 0.1 to 1 per frame. Careful choice of the integration time so that the transitions do not saturate but cover a large extent of the modulation depth can ensure consistently high contrast. It should be noted however that both methods yield a contrast of 10 dB over the wide range of settings tested here.

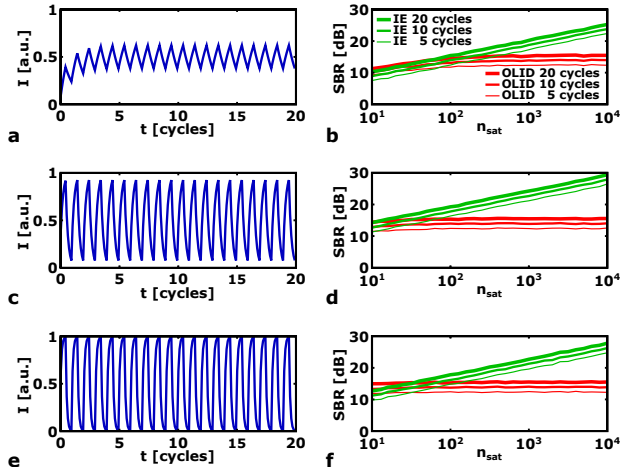

Figure S2 | Contrast evaluation. (a,c,e) Simulated fluorescence emission of a photoswitchable emitter when switched between activation and deactivation at a transition rate of 0.1, 0.5, and 1 per frame, respectively. (b,d,f) The contrast ratio between the value obtained for photo-switching and that for non-switching fluorescence emission as a function of the number of photons that would be received from at saturation ($I = 1$ in left hand panels), calculated using the first 5, 10, and 20 cycles.

Supplementary References

1. Guizar-Sicairos, M., Thurman, S. T. & Fienup, J. R. Efficient subpixel image registration algorithms. *Opt. Lett.* **33**, 156–158 (2008). doi: 10.1364/OL.33.000156.
2. Larcher, F. *et al.* A cutaneous gene therapy approach to human leptin deficiencies: correction of the murine ob/ob phenotype using leptin-targeted keratinocyte grafts. *FASEB J.* **15**, 1529–1538 (2001). doi: 10.1096/fj.1530-6860.
3. Rodriguez-Pulido, A. *et al.* Assessing the potential of photosensitizing flavoproteins as tags for correlative microscopy. *Chem. Commun.* **52**, 8405–8408 (2016). doi: 10.1039/C6CC03119F.